

The influence of titanium adhesion layer oxygen stoichiometry on thermal boundary conductance at gold contacts

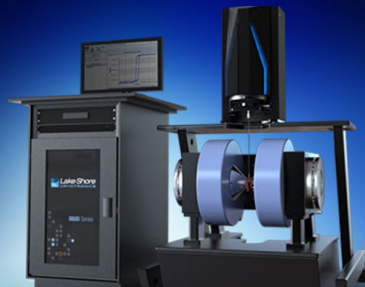
David H. Olson, Keren M. Freedy, Stephen J. McDonnell, and Patrick E. Hopkins

Citation: *Appl. Phys. Lett.* **112**, 171602 (2018); doi: 10.1063/1.5022371

View online: <https://doi.org/10.1063/1.5022371>

View Table of Contents: <http://aip.scitation.org/toc/apl/112/17>

Published by the [American Institute of Physics](#)



NEW 8600 Series VSM

For fast, highly sensitive measurement performance

LEARN MORE 

The influence of titanium adhesion layer oxygen stoichiometry on thermal boundary conductance at gold contacts

David H. Olson,¹ Keren M. Freedy,² Stephen J. McDonnell,² and Patrick E. Hopkins^{1,2,3,a)}

¹Department of Mechanical and Aerospace Engineering, University of Virginia, Charlottesville, Virginia 22904, USA

²Department of Materials Science and Engineering, University of Virginia, Charlottesville, Virginia 22904, USA

³Department of Physics, University of Virginia, Charlottesville, Virginia 22904, USA

(Received 14 January 2018; accepted 6 April 2018; published online 23 April 2018)

We experimentally demonstrate the role of oxygen stoichiometry on the thermal boundary conductance across Au/TiO_x/substrate interfaces. By evaporating two different sets of Au/TiO_x/substrate samples under both high vacuum and ultrahigh vacuum conditions, we vary the oxygen composition in the TiO_x layer from $0 \leq x \leq 2.85$. We measure the thermal boundary conductance across the Au/TiO_x/substrate interfaces with time-domain thermoreflectance and characterize the interfacial chemistry with x-ray photoemission spectroscopy. Under high vacuum conditions, we speculate that the environment provides a sufficient flux of oxidizing species to the sample surface such that one essentially co-deposits Ti and these oxidizing species. We show that slower deposition rates correspond to a higher oxygen content in the TiO_x layer, which results in a lower thermal boundary conductance across the Au/TiO_x/substrate interfacial region. Under the ultrahigh vacuum evaporation conditions, pure metallic Ti is deposited on the substrate surface. In the case of quartz substrates, the metallic Ti reacts with the substrate and getters oxygen, leading to a TiO_x layer. Our results suggest that Ti layers with relatively low oxygen compositions are best suited to maximize the thermal boundary conductance. *Published by AIP Publishing.*

<https://doi.org/10.1063/1.5022371>

The thermal resistances across heterogeneous material interfaces are well known to influence heat dissipation mechanisms in materials and devices with characteristic length scales approaching the Kapitza length, l_K , defined by $l_K = \kappa R_K = \kappa/h_K$. In this equation, κ is the thermal conductivity of a material adjacent to the interface, R_K is the thermal boundary resistance (“Kapitza resistance”),¹ and $h_K = 1/R_K$ is the thermal boundary conductance.^{2–6} Historically, understanding of the phonon transport mechanisms driving the thermal boundary conductance across interfaces has relied on the concept of energy transmission driven by the relative dissimilarities of the acoustic properties^{7,8} or phonon densities of states² intrinsic to the bulk of the two materials comprising the interface. More recently, defects and atomic disorder in the form of substrate roughness,^{9,10} dislocations,¹¹ atomic diffusion,¹² nanoscale or molecular defects,^{13,14} and structurally disordered thin films (with thicknesses $d \ll l_K$)^{9,15–18} at and near the interface have been shown to decrease h_K as compared to the corresponding “perfect” interface.⁴

Under certain conditions, the inclusion of additional interfacial moieties in the form of point defects or thin films can be used to increase the thermal boundary conductance (decrease the thermal boundary resistance). For example, our recent work has shown that point defects generated from ion irradiation can lead to increases in thermal boundary conductance¹⁵ by creating a spatial gradation of vibrational properties, similar to the so-called “vibrational bridge” effect that was computationally observed via molecular dynamics.^{19,20} As another example, the inclusion of surface adsorbates,^{21–23}

molecules,^{24,25} and adhesion layers²⁶ between a film and a substrate have been shown to increase the thermal boundary conductance across the interface. In this case, the placement of these interfacial moieties has led to stronger bonding across an otherwise relatively weakly bonded interface. The increase in bond strength then leads to an increase in thermal boundary conductance due to better coupling of high frequency phonon energies from one side of the interface to the other.^{27,28}

However, as previously mentioned, while interfacial adhesion layers and “defects”/moieties could lead to increases in the relative h_K due to bonding, the increase in interfacial disorder or additional interfaces (e.g., adhesion layers) could also lead to decreases in h_K , and this interplay between the interfacial region increasing vs. decreasing the thermal boundary conductance is relatively unstudied. For example, when molecules have been used to increase the bonding at film/substrate interfaces, and thus increase h_K , the intrinsic thermal resistance of the interfacial molecule at the junction is assumed negligible^{24,25} (i.e., heat flow through the molecule is ballistic).^{29,30} A large enough molecule at a film/substrate interface that exhibits diffusive thermal transport can lead to reductions in h_K ,^{13,31} thus counteracting any benefit of increased adhesion on thermal boundary conductance. This interplay is poorly understood and has pronounced impacts on our understanding of the intertwined role of defects and adhesion layers on the thermal boundary conductance across interfaces, along with the ability to assess and validate concepts and theories of thermal boundary conductance at strongly bonded interfaces.

Thin titanium (Ti) and TiO_x adhesion layers have been predominantly used in thin film manufacturing to increase

^{a)}phopkins@virginia.edu

interfacial bonding to a dielectric substrate. This is due to the fact that the typical Ti adhesion layer allows for an ameliorated adherence of other metal films, such as Au, Pt, Ni, and Al, to these dielectric materials. The use of these adhesion layers covers a wide array of applications, including metal contacts in electronic devices, lithium ion thin film microbatteries,^{32,33} split-ring resonators,^{34–36} and plasmon damping.^{37,38} The influence of Ti adhesion layers has also been examined for its effects on thermal transport in thin gold films on various substrates.^{26,39,40} As interfaces can become the dominant resistors in thin film systems, their thermal management is paramount in multilayer geometries, and thus, understanding the growth and chemistry mechanisms that influence the thermal performance of these adhesion layers is of the utmost importance.

In this work, we describe the results of a series of measurements across Au/non-metal substrate interfaces [amorphous silica (SiO₂), crystalline silica (quartz), sapphire (Al₂O₃), and magnesium oxide (MgO)] with TiO_x adhesion layers ranging in oxygen stoichiometries from $0 \leq x \leq 2.85$. We achieve this range of oxygen stoichiometries through the fabrication of two different sets of Au/TiO_x/substrate samples, one evaporated under high vacuum (HV) using different Ti deposition rates and the other evaporated under ultrahigh vacuum (UHV). In the UHV conditions, we identify the role of the Ti film thickness on the thermal boundary conductance, while the HV-deposited Ti demonstrates a clear dependency on the oxygen stoichiometry and hence deposition conditions. In general, our results suggest that Ti layers with relatively low oxygen compositions are best suited to maximize the thermal boundary conductance.

In the first part of this study, we fabricate the Au/TiO_x/substrate samples with electron-beam evaporation in HV. For the TiO_x layers, we evaporate Ti at 0.1, 0.5, and 1.0 Å/s in separate runs on two sets of quartz, SiO₂, MgO, and Al₂O₃ substrates. Prior to this, the quartz, SiO₂, and Al₂O₃ were sonicated in isopropanol, acetone, and methanol for 5 min each and then placed in a MARCH O₂ Plasma Etcher for 10 min. The MgO substrate was spin-cleaned with isopropanol, acetone, and methanol. After cleaning, the samples were immediately placed in the electron beam evaporator and pumped down to $\sim 10^{-6}$ Torr. Following the 3 nm Ti evaporation, we evaporate 3 nm of Au at 0.2 Å/s without breaking vacuum. The evaporator was then vented, and one of each substrate was removed to be analyzed via x-ray photoelectron spectroscopy (XPS). The evaporator was then pumped down to $\sim 10^{-6}$ Torr once again, and an additional

47 nm Au was deposited at 1 Å/s. All depositions were performed with a rotation speed of 17 rpm. XPS was used in determining the composition of the underlying TiO_x interface in the thinner sample set. X-ray reflectivity (XRR) was used to determine a thickness of ~ 50 nm Au on the thicker sample sets. As a comparison, we also evaporate 50 nm of Au on the various substrates without an adhesion layer.

XPS data were acquired with a monochromated x-ray source at a pass energy of 50 eV in a UHV system described elsewhere.⁴¹ Figure 1(a) shows XPS spectra of the O 1s core level in three distinct Ti films deposited on SiO₂ substrates at different deposition rates. The O 1s spectra are each composed of two features: a peak at 530.5 eV, corresponding to Ti-O bonds,⁴² and a broader feature at the high binding energy shoulder which is attributed to hydrocarbon species. This higher binding-energy feature decreases in intensity relative to the Ti-O state as the deposition rate is increased. The deconvolution of the spectra indicates that at 0.1 Å/s, 46% of the total oxygen signal is from Ti-O bonds. This value increases to 71% and 76% at 0.5 and 1 Å/s, respectively. The deposition rate determines the impingement rate of Ti atoms on the surface of the substrate relative to the impingement rate of residual gases in the chamber.⁴³ A cleaner interface results as Ti atoms arrive at a faster rate, allowing less opportunity for the physisorption of contaminants. Due to the constant partial pressure of oxidizing species under HV deposition conditions, the resulting Ti film is always composed primarily of oxide regardless of the deposition rate. The oxygen composition as a function of the Ti deposition rate of these high vacuum-evaporated interfaces determined via our XPS analysis is shown in Fig. 1(b). Note: this only accounts for oxygen that is bonded to Ti in the adhesion layer. We use time-domain thermoreflectance (TDTR) to measure h_K across the Au/substrate interfaces, the details of which are discussed in the [supplementary material](#).^{44–46} The values are presented only for quartz, MgO, and Al₂O₃ substrates due to a lack of sensitivity in SiO₂ samples.^{47,48}

The Au/TiO_x/substrate thermal boundary conductances as a function of x in TiO_x are plotted in Fig. 2 for the 3 nm evaporated TiO_x layers. As expected, the measured thermal boundary conductances across the Au/TiO_x/substrate interfaces are higher than the Au/substrate interfaces without the adhesion layer (in most cases, more than a factor of three higher), which is most likely a consequence of increased adhesion between the Au and the substrate and consistent with previous results.²⁶ In general, we observe a reduction in h_K with an increase in the oxygen composition in the TiO_x

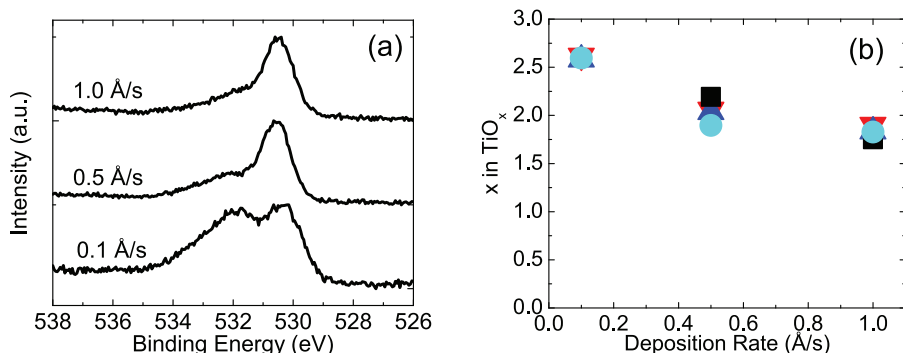


FIG. 1. (a) O 1s core level binding energies of the Ti adhesion layer on an SiO₂ substrate and (b) oxygen content in the TiO_x adhesion layer as a function of the Ti deposition rate for quartz (squares), SiO₂ (circles), Al₂O₃ (downward facing triangles), and MgO (upward facing triangles). The value of Ti deposited on the quartz substrate at 0.1 Å/s could not be recovered due to sample size restrictions in XPS analysis for (b).

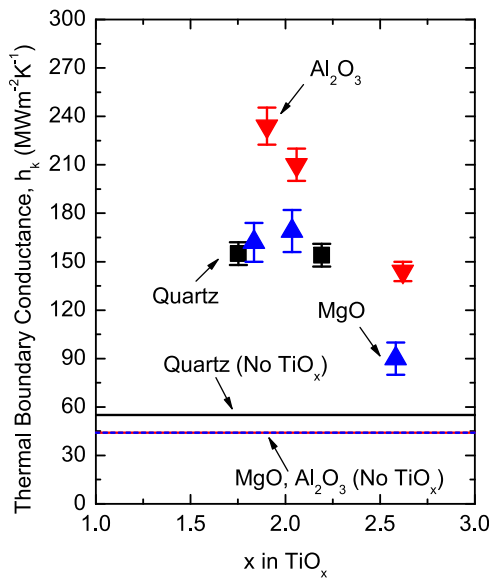


FIG. 2. Thermal boundary conductances across the Au/TiO_x/substrate deposited using electron-beam evaporation under high vacuum. The thermal boundary conductance of the quartz sample with Ti deposited at 0.1 Å/s is not shown because the stoichiometry could not be determined due to sample size limitations. Despite this, h_K was determined to be 130 MW m⁻² K⁻¹ for that sample, relatively consistent with the other quartz substrate samples. The lines are the measured data from the Au/substrate samples with no TiO_x adhesion layers.

layer for the MgO and Al₂O₃ substrates. Since the oxygen composition is directly related to the deposition rate in our evaporator, an initial qualitative conclusion is that under typical HV conditions, the deposition rate of evaporated Ti will result in TiO_x with varying x , and a higher oxygen composition in this evaporated adhesion layer leads to a lower h_K across the Au/TiO_x/MgO and Au/TiO_x/Al₂O₃ interfaces. While in most of these cases TiO_x offers an improved h_K as compared to the thermal boundary conductance across the Au/substrate interface without the adhesion layer, for the case of the largest oxygen composition $x = 2.85$, the impact of the adhesion layer loses its pronounced benefit in terms of increasing h_K . The thermal boundary conductance across this Au/TiO_{2.85}/MgO interface is about a factor of two higher than the Au/MgO case, while for lower oxygen compositions in the evaporated TiO_x adhesion layer, the improvement in thermal boundary conductance is a factor of three to four times higher.

Another feature we observe in Fig. 2 is that the thermal boundary conductance across the Au/TiO_x/quartz is independent of x . There could be several mechanisms at play which cause this different trend in h_K vs. x for the quartz substrate as compared to MgO and Al₂O₃, including reduction of the deposited Ti and differing TiO_x film qualities and morphologies. The variabilities and vacuum levels of this evaporator prevent us from making more quantitative conclusions on these particular samples beyond our initial qualitative conclusion related to the processing, chemical composition, and thermal boundary conductance, discussed above. However, we gain more insight into this relationship by repeating this study with UHV-grown titanium adhesion layers. In this case, due to the UHV conditions in our chamber, the reduced physisorption of foreign species is correlated with a decrease in oxidized Ti at the substrate.

The Ti adhesion layers were deposited in UHV (7.5×10^{-10} Torr) via electron-beam evaporation on the same aforementioned substrates using identical cleaning procedures. Samples were subsequently coated with a thin layer of gold *in situ* to prevent oxidation of the underlying Ti layer.⁴³ The gold was deposited until the XPS signal of the substrate is buried, and its thickness was later confirmed with XRR. The samples were immediately transferred to the HV evaporator and pumped down to $\sim 10^{-6}$ Torr to be deposited with a thicker Au layer (47 nm). A comparison of the Ti 2*p* spectra for Ti deposited at 1.0 Å/s in HV and Ti deposited at <0.1 Å/s under UHV is shown in Fig. 1 of the [supplementary material](#). In the HV-deposited sample, metallic Ti accounts for only 6% of the total Ti signal and the remainder is from TiO₂. In contrast, Ti deposited in UHV appears purely metallic.

The measured thermal boundary conductances as a function of the Ti layer thickness are shown in Fig. 3. In the cases of Al₂O₃ and MgO, there is a clear increase in h_K with increasing Ti thickness. On the other hand, as the thickness of Ti increases on the quartz substrate, the thermal boundary conductance remains relatively constant. An increase in thermal boundary conductance (decrease in thermal boundary resistance) with an increase in the film thickness suggests that the Ti film is not in a fully thermally diffusive regime, and thus at least partially ballistic electron and/or phonon transport of carriers emitted from the Au is occurring in the Ti layer. This is the case in Al₂O₃ and MgO for the Ti thicknesses presented here. However, to explain the phenomena observed in the quartz substrate, we must examine the free energies of the Mg-O, Al-O, and Si-O bonds. As the Ti-O bond has a smaller free energy compared to Mg-O and Al-O bonds,⁴⁹ Ti near the substrate will not break these bonds to form TiO_x. On the other hand, the free energy associated with the Ti-O bond is smaller than that of Si-O, suggesting that Si-O bonds near the interface break to form TiO_x. This

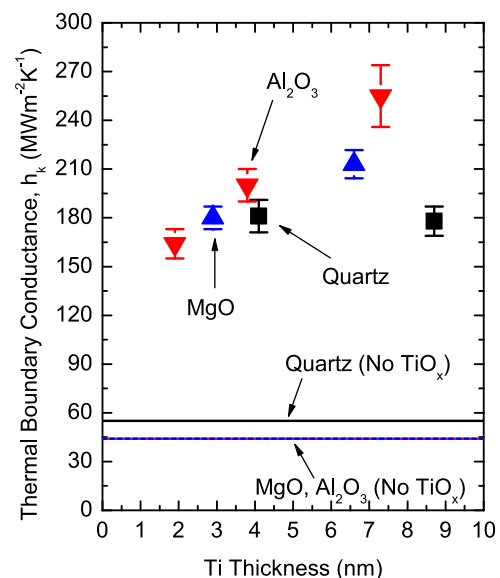


FIG. 3. Thermal boundary conductances at Au/substrate interfaces with a Ti adhesion layer deposited via electron-beam evaporation in UHV as a function of the Ti thickness. The lines are the measured data from the Au/substrate samples with no Ti adhesion layer.

is confirmed via XPS, shown in Fig. 4, the data of which exhibit bond scission in SiO₂ and quartz substrates but not in MgO and Al₂O₃. The Si 2*p* spectra shown in Figs. 4(a) and 4(b) indicate that in UHV, Ti reacts with oxygen from the substrate, which leads to the appearance of the Si⁰ chemical state.

With this additional information, we revisit h_K in the HV evaporated quartz samples. Regardless of the deposition rate, the conductance across the Au/TiO_x/quartz interface is not altered significantly across oxygen stoichiometries. Based on XPS data from UHV grown samples, Ti deposited onto quartz and SiO₂ breaks the Si-O bond to form Ti-O, presenting similar bonding across the Au/TiO_x/quartz interface. This is confirmed further in Ti grown under UHV conditions on quartz, whereby h_K is not altered significantly. We currently do not understand why increasing the thickness of the Ti at this interface does not change h_K . However, we note that since the UHV grown Ti is not purely metallic on this substrate, an increased contribution from vibrational transport will most certainly be playing a role compared to the pure Ti case.

There are a variety of factors that could alter our presented values for thermal boundary conductances at these interfaces. Differences in UHV and HV deposition parameters, for example, have the potential to alter the structure of the TiO_x adhesion layer. In turn, differences in the structure can alter measured thermal boundary conductances, which could explain differences across deposition rates in HV-deposited adhesion layers and the increase in h_K for UHV samples. Additionally, we cannot confirm that a conformal adhesion layer was deposited with a constant thickness. Indeed, we account for the uncertainty of the thickness

of the Ti adhesion layer in our analysis of thermal boundary conductance, but this does not account for islanding or other complications arising due to electron-beam evaporated metals. We can conclude, however, that Ti adhesion layers deposited in UHV in general improve heat management compared to their HV counterparts, especially as the deposition rate of the Ti is lowered.

In summary, we report on a series of measurements demonstrating the role of oxygen stoichiometry on the thermal boundary conductance across Au/TiO_x/substrate interfaces. Under HV conditions, where the evaporated Ti oxidizes upon reaching the substrate, we show that slower deposition rates correspond to a higher oxygen content in the TiO_x layer, which results in a lower thermal boundary conductance across the Au/TiO_x/substrate interfacial region. Under UHV conditions, pure metallic Ti is deposited on the substrate surface. In the case of quartz substrates, the metallic Ti reacts with the substrate and getters oxygen, leading to a TiO_x layer. For the cases of Al₂O₃ and MgO, we demonstrate that h_K is dependent on the thickness of the adhesion layer. In general, our results suggest that Ti layers with relatively low oxygen compositions are best suited to maximize the thermal boundary conductance.

See [supplementary material](#) for details including the choice of adhesion layer deposition rates, calculation of the adhesion layer stoichiometries and thicknesses, a description of TDTR, and a comparison of the XPS spectra of Ti deposited in HV and UHV.

D. H. Olson would like to thank the Virginia Space Grant Consortium (VSGC) for their continued funding and support. We also appreciate the support from the Army Research Office, Grant Nos. W911NF-16-1-0320 and W911NF-16-1-0406.

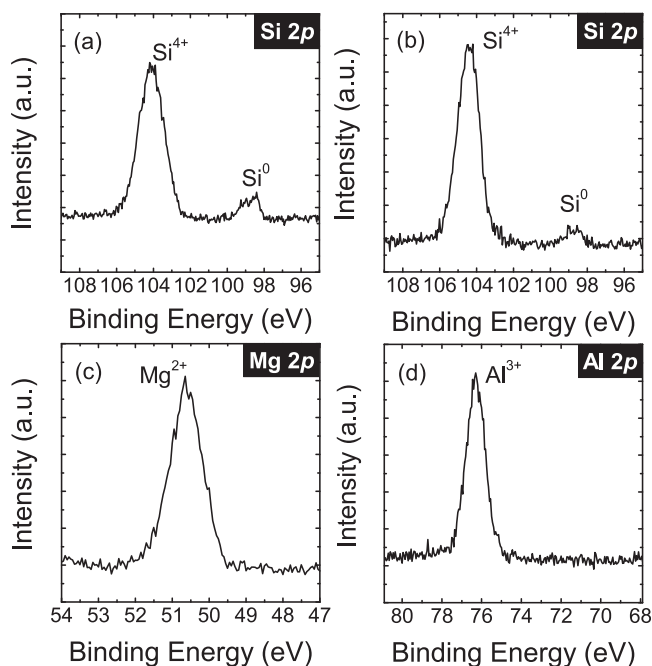


FIG. 4. Si 2*p* spectra of (a) SiO₂ and (b) quartz, (c) Mg 2*p* spectra of MgO, and (d) Al 2*p* spectra of Al₂O₃ after depositing a thin layer of Ti in UHV. In (a) and (b), the reaction of Ti with oxygen from these substrates leads to the appearance of the Si⁰ chemical state, while the lack of Mg⁰ and Al⁰ states in (c) and (d), respectively, suggests no reaction of Ti with oxygen from these substrates.

¹P. L. Kapitza, Zh. Eksp. Teor. Fiz. **11**, 1 (1941).

²E. T. Swartz and R. O. Pohl, *Rev. Mod. Phys.* **61**, 605 (1989).

³D. G. Cahill, W. K. Ford, K. E. Goodson, G. D. Mahan, A. Majumdar, H. J. Maris, R. Merlin, and S. R. Phillpot, *J. Appl. Phys.* **93**, 793 (2003).

⁴P. E. Hopkins, *ISRN Mech. Eng.* **2013**, 682586.

⁵D. G. Cahill, P. V. Braun, G. Chen, D. R. Clarke, S. Fan, K. E. Goodson, P. Keblinski, W. P. King, G. D. Mahan, A. Majumdar *et al.*, *Appl. Phys. Rev.* **1**, 011305 (2014).

⁶C. Monachon, L. Weber, and C. Dames, *Annu. Rev. Mater. Res.* **46**, 433 (2016).

⁷W. A. Little, *Can. J. Phys.* **37**, 334 (1959).

⁸J. D. N. Cheeke, H. Ettinger, and B. Hebral, *Can. J. Phys.* **54**, 1749 (1976).

⁹P. E. Hopkins, L. M. Phinney, J. R. Serrano, and T. E. Beechem, *Phys. Rev. B* **82**, 085307 (2010).

¹⁰J. C. Duda and P. E. Hopkins, *Appl. Phys. Lett.* **100**, 111602 (2012).

¹¹P. E. Hopkins, J. C. Duda, S. P. Clark, C. P. Hains, T. J. Rotter, L. M. Phinney, and G. Balakrishnan, *Appl. Phys. Lett.* **98**, 161913 (2011).

¹²P. E. Hopkins, P. M. Norris, R. J. Stevens, T. Beechem, and S. Graham, *J. Heat Transfer* **130**, 062402 (2008).

¹³J. T. Gaskins, A. Bulusu, A. J. Giordano, J. C. Duda, S. Graham, and P. E. Hopkins, *J. Phys. Chem. C* **119**, 20931 (2015).

¹⁴P. E. Hopkins, J. C. Duda, C. W. Petz, and J. A. Floro, *Phys. Rev. B* **84**, 035438 (2011).

¹⁵C. S. Gorham, K. Hattar, R. Cheaito, J. C. Duda, J. T. Gaskins, T. E. Beechem, J. F. Ihlefeld, L. B. Biedermann, E. S. Piekos, D. L. Medlin, and P. E. Hopkins, *Phys. Rev. B* **90**, 024301 (2014).

¹⁶P. E. Hopkins, K. Hattar, T. Beechem, J. F. Ihlefeld, D. L. Medlin, and E. S. Piekos, *Appl. Phys. Lett.* **98**, 231901 (2011).

¹⁷P. E. Hopkins, T. E. Beechem, J. C. Duda, K. Hattar, J. F. Ihlefeld, M. A. Rodriguez, and E. S. Piekos, *Phys. Rev. B* **84**, 125408 (2011).

- ¹⁸P. E. Hopkins, K. Hattar, T. Beechem, J. F. Ihlefeld, D. L. Medlin, and E. S. Piekos, *Appl. Phys. Lett.* **101**, 099903 (2012).
- ¹⁹J. C. Duda, T. S. English, E. S. Piekos, T. E. Beechem, T. W. Kenny, and P. E. Hopkins, *J. Appl. Phys.* **112**, 073519 (2012).
- ²⁰T. S. English, J. C. Duda, J. L. Smoyer, D. A. Jordan, P. M. Norris, and L. V. Zhigilei, *Phys. Rev. B* **85**, 035438 (2012).
- ²¹P. E. Hopkins, M. Baraket, E. V. Barnat, T. E. Beechem, S. P. Kearney, J. C. Duda, J. T. Robinson, and S. G. Walton, *Nano Lett.* **12**, 590 (2012).
- ²²B. M. Foley, S. C. Hernández, J. C. Duda, J. T. Robinson, S. G. Walton, and P. E. Hopkins, *Nano Lett.* **15**, 4876 (2015).
- ²³S. Walton, B. Foley, S. Hernández, D. Boris, M. Baraket, J. Duda, J. Robinson, and P. Hopkins, in *59th Annual Technical Conference on Society of Vacuum Coaters* [Surf. Coat. Technol. **314**, 148 (2017)].
- ²⁴M. D. Losego, M. E. Grady, N. R. Sottos, D. G. Cahill, and P. V. Braun, *Nat. Mater.* **11**, 502 (2012).
- ²⁵P. J. O'Brien, S. Shenogin, J. Liu, P. K. Chow, D. Laurencin, P. H. Mutin, M. Yamaguchi, P. Koblinski, and G. Ramanath, *Nat. Mater.* **12**, 118 (2013).
- ²⁶J. C. Duda, C.-Y. P. Yang, B. M. Foley, R. Cheaito, D. L. Medlin, R. E. Jones, and P. E. Hopkins, *Appl. Phys. Lett.* **102**, 081902 (2013).
- ²⁷J. C. Duda, T. S. English, E. S. Piekos, W. A. Soffa, L. V. Zhigilei, and P. E. Hopkins, *Phys. Rev. B* **84**, 193301 (2011).
- ²⁸A. Giri, J. L. Braun, and P. E. Hopkins, *J. Phys. Chem. C* **120**, 24847 (2016).
- ²⁹Z. Wang, J. A. Carter, A. Lagutchev, Y. K. Koh, N. H. Seong, D. G. Cahill, and D. D. Dlott, *Science* **317**, 787 (2007).
- ³⁰Z. Wang, D. G. Cahill, J. A. Carter, Y. K. Koh, A. Lagutchev, N. H. Seong, and D. D. Dlott, *Chem. Phys.* **350**, 31 (2008).
- ³¹A. Giri, J.-P. Niemelä, T. Tynell, J. T. Gaskins, B. F. Donovan, M. Karppinen, and P. E. Hopkins, *Phys. Rev. B* **93**, 115310 (2016).
- ³²E. M. F. Vieira, J. F. Ribeiro, R. Sousa, M. M. Silva, L. Dupont, and L. M. Gonçalves, *J. Electron. Mater.* **45**, 910 (2016).
- ³³S. Hsieh, D. Beck, T. Matsumoto, and B. E. Koel, *Thin Solid Films* **466**, 123 (2004).
- ³⁴B. Lahiri, R. Dylewicz, R. M. D. L. Rue, and N. P. Johnson, *Opt. Express* **18**, 11202 (2010).
- ³⁵C. Jeppesen, N. A. Mortensen, and A. Kristensen, *Appl. Phys. Lett.* **97**, 263103 (2010).
- ³⁶E. Ekmekci, A. C. Strikwerda, K. Fan, G. Keiser, X. Zhang, G. Turhan-Sayan, and R. D. Averitt, *Phys. Rev. B* **83**, 193103 (2011).
- ³⁷H. Aouani, J. Wenger, D. Gérard, H. Rigneault, E. Devaux, T. W. Ebbesen, F. Mahdavi, T. Xu, and S. Blair, *ACS Nano* **3**, 2043 (2009).
- ³⁸T. G. Habteyes, S. Dhuey, E. Wood, D. Gargas, S. Cabrini, P. J. Schuck, A. P. Alivisatos, and S. R. Leone, *ACS Nano* **6**, 5702 (2012).
- ³⁹A. Giri, J. T. Gaskins, B. F. Donovan, C. Szejewski, R. J. Warzoha, M. A. Rodriguez, J. Ihlefeld, and P. E. Hopkins, *J. Appl. Phys.* **117**, 105105 (2015).
- ⁴⁰K. M. Freedy, A. Giri, B. M. Foley, M. R. Barone, P. E. Hopkins, and S. McDonnell, *Nanotechnol.* **29**(14), 145201 (2017).
- ⁴¹K. M. Freedy, P. M. Litwin, and S. J. McDonnell, *ECS Trans.* **77**, 11 (2017).
- ⁴²T. Sham and M. Lazarus, *Chem. Phys. Lett.* **68**, 426 (1979).
- ⁴³S. McDonnell, C. Smyth, C. L. Hinkle, and R. M. Wallace, *ACS Appl. Mater. Interfaces* **8**, 8289 (2016).
- ⁴⁴A. J. Schmidt, X. Chen, and G. Chen, *Rev. Sci. Instrum.* **79**, 114902 (2008).
- ⁴⁵P. E. Hopkins, J. R. Serrano, L. M. Phinney, S. P. Kearney, T. W. Grasser, and C. T. Harris, *J. Heat Transfer* **132**, 081302 (2010).
- ⁴⁶D. G. Cahill, *Rev. Sci. Instrum.* **75**, 5119 (2004).
- ⁴⁷J. L. Braun, C. H. Baker, A. Giri, M. Elahi, K. Artyushkova, T. E. Beechem, P. M. Norris, Z. C. Leseman, J. T. Gaskins, and P. E. Hopkins, *Phys. Rev. B* **93**, 140201 (2016).
- ⁴⁸C. J. Szejewski, N. C. Creange, K. Sun, A. Giri, B. F. Donovan, C. Constantini, and P. E. Hopkins, *J. Appl. Phys.* **117**, 084308 (2015).
- ⁴⁹P. Atkins and J. De Paula, *Thermodynamics and Kinetics* (W. H. Freeman and Company, 2005).